NONLINEAR MODELS AND METHODS FOR SPACE-OBJECT IMAGING THROUGH ATMOSPHERIC TURBULENCE

Timothy J. Schulz

Department of Electrical Engineering
Michigan Technological University
Houghton, MI 49931-1295 USA
schulz@mtu.edu

ABSTRACT

In this paper a nonlinear model is presented for the problem of space-object imaging through atmospheric turbulence, and a nonlinear method is discussed for forming fine-resolution images from blurred telescope data. Results from real telescope data are also presented.

1. INTRODUCTION

The angular resolution of an optical telescope under ideal circumstances is determined by the ratio of the light's wavelength to the telescope's diameter. A 1.6 meter ground-based telescope sensing green light, for example, should resolve features on the order of 10 inches when observing the Hubble Space Telescope in its 600 km orbit. Time-varying changes in the refractive index of Earth's atmosphere can, however, swell this resolution by a factor of 15 making meaningful inference about the satellite from ground-based pictures nearly impossible. This "seeing" problem has plagued astronomers for years.

One approach to correcting the seeing problem is accomplished through the use of signal processing techniques: a sequence of short-exposure images is recorded and the turbulence-induced blurs are removed through post-detection processing. The blurring model that relates the unknown object function to the data is linear; however, the point-spread functions for each short-exposure image are neither typically know nor easily predicted, and the parameters that determine these blurring functions enter into the problem in a highly nonlinear manner. In addition, the nonnegativity constraint on the unknown object function leads to the utilization of nonlinear restoration methods even when the point-spread functions are known.

2. SYSTEM MODEL

Incoherent imaging systems such as photographic cameras, microscopes, and telescopes are usually well modeled as linear, space-invariant systems [2], and the imagery acquired by these systems is often consistent with the following model:

$$i(y) = \int h(y-x)o(x)dx, \qquad (1)$$

where y and x are two-dimensional spatial variables, $i(\cdot)$ is the intensity image recorded by the instrument, $h(\cdot)$ is the imaging system's point-spread function (or impulse response), and $o(\cdot)$ is the intensity distribution of light that is reflected by, emitted from, or transmitted through a remote object or scene of interest[1]. The point-spread functions for many systems are induced by the optical elements used to collect and focus the light. The mathematical basis for the determination of these functions is provided by techniques from Fourier optics [2]. For an ideal, single-lens imaging system operating in perfect focus with narrowband light, the point-spread func-

[1] Actually, $o(\cdot)$ represents the object's intensity distribution *scaled* by the system magnification factor.

tion is mathematically determined by:

$$h(y) = \left| \int P(u) e^{-j\frac{2\pi}{\lambda f} y \cdot u} du \right|^2, \qquad (2)$$

where:

- u is a spatial variable in the system's pupil plane;
- $P(\cdot)$ is the system *pupil function*, which takes a value of 1 within the lens aperture and 0 otherwise;
- λ is the nominal wavelength of the light; and
- f is the lens focal length.

For a circular aperture of diameter D, the corresponding point-spread function has the mathematical form:

$$h(y) = \left| \frac{J_1[2\pi D|y|/(\lambda f)]}{D|y|/(\lambda f)} \right|^2, \qquad (3)$$

where $J_1[\cdot]$ is a Bessel function of the first kind, order 1.

For systems with optical aberrations or focusing errors, the pupil function can often be conveniently modified to a *generalized pupil function*:

$$\mathcal{P}(u) = P(u) e^{j\theta(u)}, \qquad (4)$$

where $\theta(\cdot)$ is the wavefront phase error induced by the aberrations or focusing errors. The point-spread function, then, is modeled as

$$\begin{aligned} h(y;\theta) &= \left| \int \mathcal{P}(u) e^{-j\frac{2\pi}{\lambda f} y \cdot u} du \right|^2 \\ &= \left| \int P(u) e^{j\theta(u)} e^{-j\frac{2\pi}{\lambda f} y \cdot u} du \right|^2, \end{aligned} \qquad (5)$$

where the notation $h(y;\theta)$ shows the point spread function's dependence on the wavefront phase error $\theta(\cdot)$.

Wave propagation through an inhomogeneous medium such as Earth's atmosphere can also cause the point-spread function for an optical system to become distorted in a manner similar to optical aberrations and focusing errors. That is, the effects of atmospheric turbulence are often modeled by including a time-varying phase error into the system's generalized pupil function:

$$\mathcal{P}(u;\theta_t) = P(u) e^{j\theta_t(u)}, \qquad (6)$$

so that the system is characterized by a time-varying point-spread function:

$$h(y;\theta_t) = \left| \int P(u) e^{j\theta_t(u)} e^{-j\frac{2\pi}{\lambda f} y \cdot u} du \right|^2. \qquad (7)$$

The time-varying phase errors $\theta_t(\cdot)$ are caused by inhomogeneous temperature fluctuations in Earth's atmosphere, which in turn induce time- and space-varying fluctuations in the atmosphere's refractive index. The correlation scales for these fluctuations in both time and space depend on many physical factors that characterize the atmosphere; however, correlation times of a few milliseconds and correlation lengths of a few centimeters are common. Larger correlation times and lengths are characteristic of weak turbulence.

For many operational systems, it is common to acquire a sequence of images, each being recorded with an exposure time that is short compared with the fluctuation time of the atmosphere. Provided that the object intensity does not change between exposures, the recorded imagery is then modeled as:

$$i(y;\theta_{t_k}, o) = \int h(y - x;\theta_{t_k}) o(x) dx, \qquad (8)$$

where $\theta_{t_k}(\cdot)$ is the atmospheric phase associated with the kth short exposure image, and the notation $i(\cdot;\theta_{t_k}, o)$ shows the explicit dependence of the image intensity on both the atmospheric phase error $\theta_{t_k}(\cdot)$ and on the unknown object intensity $o(\cdot)$.

3. DATA MODEL

The data recorded by a typical imaging system are directly related to the image intensity $i(\cdot;\theta_{t_k}, o)$; however, this intensity is typically sampled by an array of discrete detector elements and the recorded data are further subject to the effects of internal and external background counts, nonuniform camera response, and other sources of camera noise. A common data model is then:

$$d_k[n] = N_k[n] + M_k[n] + g_k[n] + b[n], \qquad (9)$$

where

- n is a two-dimensional, discrete index to elements of the camera's detector array;
- $N_k[n]$ is the number of object-induced photoelectrons recorded by the nth detector element during the kth exposure;
- $M_k[n]$ is the number of internal and external background photoelectrons recorded by the nth detector element during the kth exposure;
- $g_k[n]$ is the signal-independent detector noise for the nth detector, usually induced by the detector's electronics; and
- $b[n]$ is a deterministic bias.

In addition, the data are usually statistically independent across detector elements.

The number of object-induced photoelectrons recorded by the nth detector element is usually modeled as a Poisson random variable whose mean is

$$E\{N_k[n]\} = a[n] \int_{\mathcal{Y}_n} i(y; \theta_k, o) dy, \qquad (10)$$

where $\mathcal{Y}_n$ is the spatial region over which the nth detector element acquires data, and $a[n]$ is a nonnegative gain parameter that accounts for the efficiency (possibly nonuniform) of the detector elements. For many systems, the image intensity varies slowly with respect to the regions $\{\mathcal{Y}_n\}$, and the integrating operation is approximated by a sampling operation:

$$E\{N_k[n]\} \simeq |\mathcal{Y}_n| a[n] i(y_n; \theta_k, o), \qquad (11)$$

where y_n and $|\mathcal{Y}_n|$ denote the location and area, respectively, of the nth detector element. Furthermore, the object function is often approximated over a discrete grid so that the integral relating the image intensity to the object function is approximated by the summation:

$$i(y_n; \theta_k, o) = \sum_m h(y_n - x_m; \theta_k) o(x_m), \qquad (12)$$

and the object samples at the discrete sample points $\{x_n\}$ are the parameters to be estimated. The number of background-induced photoelectrons acquired by the nth detector element is also a Poisson random variable with the mean $i_b[n]$, and the detector noise $g_k[n]$ is usually modeled as a zero-mean Gaussian variable with variance $\sigma^2[n]$. The background mean $i_b[n]$, detector noise variance $\sigma^2[n]$, and deterministic bias $b[n]$ are usually determined through a controlled calibration procedure.

Because Eq. (9) contains a mixture of Poisson and Gaussian random variables, the probability density for the measured data is a complicated function that involves an infinite sum [4], [3]. If, however, the CCD read-out noise variance is large[2], then the pre-processed data:

$$\tilde{d}_k[n] = d_k[n] - b[n] + \sigma^2[n], \qquad (13)$$

are approximately Poisson distributed with the mean function

$$E\{\tilde{d}_k[n]\} = i(y_n; \theta_k, o) + \sigma^2[n]. \qquad (14)$$

4. MAXIMUM-LIKELIHOOD ESTIMATION

If the unknown object function at the sample points $\{x_m\}$ and phase errors $\theta_k(\cdot)$ are all treated as deterministic, but unknown, parameters, then the method of maximum-likelihood estimation can be applied for the simultaneous estimation of the unknown object and phase errors. Note that the phase errors are related to the data mean in a highly nonlinear manner. This, coupled with the fact that the object intensity must be a nonnegative function, makes the estimation of the phase errors and object intensity a highly nonlinear problem.

A numerical algorithm based on the expectation-maximization (EM) method [6] has been described in [1] and [7] for solving this estimation problem. The results of applying this method to real telescope data are summarized in the following section.

5. RESULTS WITH REAL DATA

Telescope data were acquired by the Air Force Maui Optical Station (AMOS) on March 9, 1995

[2] See, for example, Ref. [5].

Table 1: Telescope and imaging system parameters for the ground-based imagery of the Hubble Space Telescope.

Aperture diameter:	1.6 m
Field-of-view:	6 arc seconds
Detector sampling:	128 × 128
Exposure time:	8 ms per exp.
Object photoelectrons:	2.8 million per exp.
Background photoelectrons:	0.5 million per exp.
CCD read-out noise:	9 photoelectrons rms
CCD conversion factor:	7 photoelectrons/count
Exposures per restoration	16 (656 exposures total)

and subsequently processed by the technique described in [1] and [7]. The telescope and imaging system parameters are listed in Table 1. The telescope's observations were of the Hubble Space Telescope in its 600 km orbit. 656 image frames were taken with an 8 ms exposure time; four of these images are shown in Figure 1. The 656 images were partitioned into 41 sets of 16, and each set in the partition was used to obtain one object restoration. Four of these restorations are shown in Figure 2. Each restoration required approximately 15 minutes of processing on 9 nodes of an IBM SP2 at the Maui High Performance Computing Center.

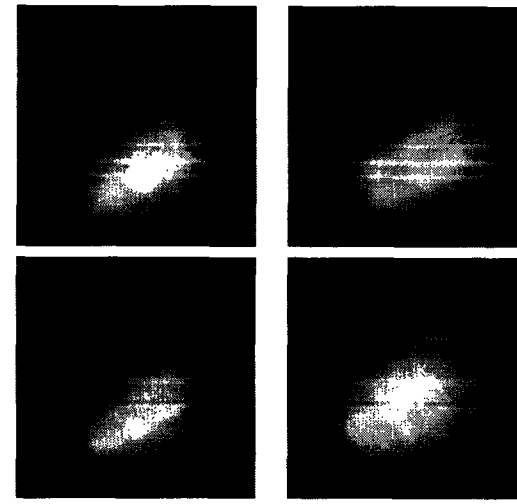

Figure 1: Four short exposure images of the Hubble Space Telescope acquired with a ground based telescope.

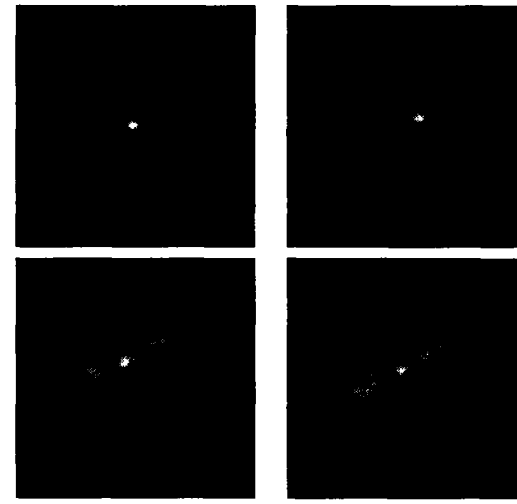

Figure 2: Four restored images of the Hubble Space Telescope.

6. SUMMARY

A nonlinear model has been developed for the problem of space-object imaging through atmospheric turbulence, and a nonlinear, maximum-likelihood estimation method has been described for forming fine-resolution images from blurred telescope data. Current work on this problem includes: a reduction of the computation time by a more efficient utilization of the processing architecture, and through the utilization of numerical methods with faster convergence rates; and the use of image models and phase-aberration priors for improved robustness in low-light (high noise) situations.

7. REFERENCES

[1] T. J. Schulz, "Multi-frame blind deconvolution of astronomical images", *J. Opt. Soc. Am. A*, Vol. 10, pp. 1064-1073, 1993.

[2] J. W. Goodman, *Introduction to Fourier Optics*, 2nd edition, McGraw-Hill, New York, 1996.

[3] D. L. Snyder, C. W. Helstrom, A. D. Lanterman, M. Faisal, and R. L. White, "Compensation for readout noise in CCD images", *J. Opt. Soc. Am. A*, Vol. 12, pp. 272-283, 1995.

[4] D. L. Snyder, A. M. Hammoud, and R. L. White, "Image recovery from data acquired with a charge-coupled-device camera", *J. Opt. Soc. Am. A*, Vol. 10, pp. 1014-1023, 1993.

[5] W. Feller, *An Introduction to Probability Theory and Its Applications*, John Wiley, New York, 1968.

[6] A. P. Dempster, N. M. Laird and D. B. Rubin, "Maximum likelihood from incomplete data via the EM algorithm", J. R. Stat. Soc. B, Vol. 39, pp. 1-37, 1977.

[7] T. J. Schulz, J. J. Miller, and B. E. Stribling, "Phase-error correction through multiframe blind deconvolution", Proc. of the 1996 IEEE International Conference on Image Processing, Lausanne, Switzerland, September, 1996.